Towards a parameter-free calculation of the nuclear matrix element for the $0\nu\beta\beta$ decay

Luigi Coraggio

Istituto Nazionale di Fisica Nucleare - Sezione di Napoli

9 marzo 2017

Acknowledgements

- L. De Angelis (INFN-NA)
- T. Fukui (INFN-NA
- A. Gargano (INFN-NA)
- N. Itaco (SUN and INFN-NA)
- L. C. (INFN-NA)

Summary

- The neutrinoless double-β decay
- The problematics of the calculation of the nuclear matrix element (NME) of $0\nu\beta\beta$ decay
- Nuclear structure calculations of the NME
- The realistic nuclear shell model
- Testing the theoretical framework: calculation of the GT strengths and the nuclear matrix element of $2\nu\beta\beta$ decay
- Conclusions and outlook

The detection of the $0\nu\beta\beta$ decay is nowadays one of the main targets in many laboratories all around the world, triggered by the search of ”new physics” beyond the Standard Model.

- Its detection
  - would correspond to a violation of the conservation of the leptonic number,
  - may provide more informations on the nature of the neutrinos (the neutrino as a Majorana particle, determination of its effective mass, ..).

The double β-decay

The semiempirical mass formula provides two different parabolas for even-mass isobars:

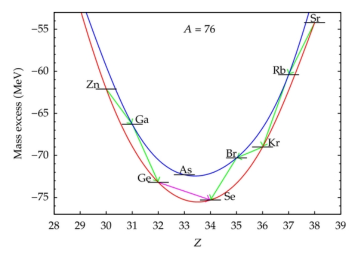

- Maria Goeppert-Mayer (1935) suggested the possibility to detect $(A, Z) \rightarrow (A, Z+2) + e^- + e^- + \overline{\nu}_e + \overline{\nu}_e$
- Historically, Giulio Racah was the first one, to test the neutrino as a Majorana particle, to consider the process: $(A, Z) \rightarrow (A, Z+2) + e^- + e^-$

The neutrinoless double β-decay

The inverse of the $0\nu\beta\beta$-decay half-life is proportional to the squared nuclear matrix element (NME).
This evidences the relevance to calculate the NME

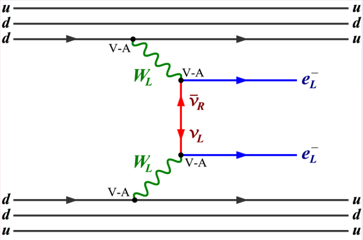

$$\left[T^{0\nu}_{1/2}\right]^{-1} = G^{0\nu} \left|M^{0\nu}\right|^2 \langle m_\nu \rangle^2 \quad ,$$

- $G^{0\nu}$ is the so-called phase-space factor, obtained by integrating over she single electron energies and angles, and summing over the final-state spins;
- $\langle m_\nu \rangle = \mid \sum_k m_k U^2_{ek} \mid$ effective mass of the Majorana neutrino, U_{ek} being the lepton mixing matrix.

The detection of the $0\nu\beta\beta$-decay

It is necessary to locate the nuclei that are the best candidates to detect the $0\nu\beta\beta$-decay

- The main factors to be taken into account are:
  - the Q-value of the reaction;
  - the phase-space factor $G^{0\nu}$;
  - the isotopic abundance

The detection of the $0\nu\beta\beta$-decay

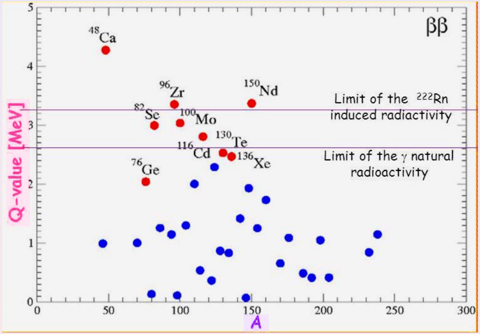

- First group: ^{76}Ge, ^{130}Te, and ^{136}Xe.
- Second group: ^{82}Se, ^{100}Mo, and ^{116}Cd.
- Third group: ^{48}Ca, ^{96}Zr, and ^{150}Nd.

GERDA@LNGS

- High purity enriched Ge crystal diodes (HPGe) as a beta decay source and particle detector.
- The detector array is suspended in a liquid argon cryostat lined with copper and surrounded by an ultra-pure water tank.
- The collaboration predicts less than one event each year per kilogram of material. A narrow spike around the $0\nu\beta\beta$ Q-value= 2039 keV is expected.

LUCIFER@LNGS

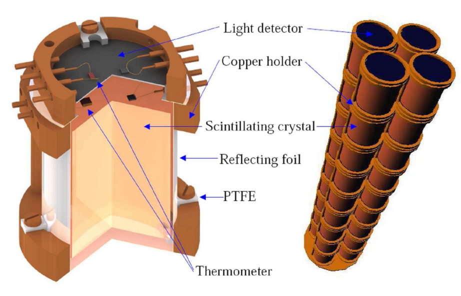

- Scintillating bolometers of ZnSe are the baseline choice of the LUCIFER experiment, whose aim is to observe the neutrinoless double beta decay of ^{82}Se.
- The bolometer is a 431 g ZnSe crystal with cylindrical shape (height 44.3 mm and diameter 48.5 mm).
- This experiment aims at a background lower than 10^{-3} counts/keV/kg/y in the energy region of the $0\nu\beta\beta$-decay of 82Se.

CUORE@LNGS

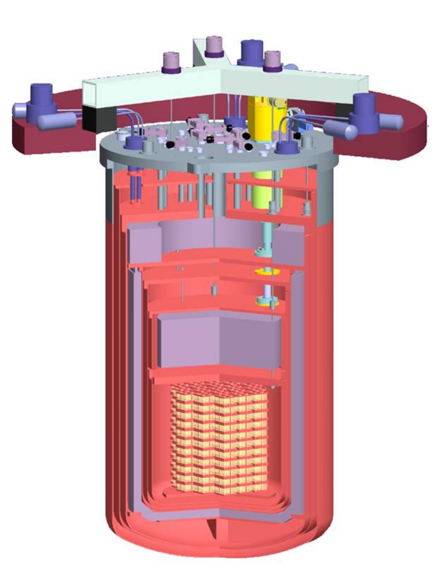

- TeO_2 crystals used as low heat capacity bolometers, arranged into towers and cooled in a large cryostat to approximately 10 m°K with a dilution refrigerator.
- The detectors are isolated from backgrounds by ultrapure low-radioactivity shielding.
- Temperature spikes from electrons emitted in Te $0\beta\beta$ are collected for spectrum analysis.

The calculation of the NME

The NME is given by

$$M^{0\nu} = M^{0\nu}_{GT} - \left(\frac{g_V}{g_A}\right)^2 M^{0\nu}_{F} - M^{0\nu}_{T} \quad ,$$

where the matrix elements are defined as follows:

$$M^{0\nu}_{\alpha} = \sum_{m,n} \langle 0^+_f \mid \tau^-_m \tau^-_n O^{\alpha}_{mn} \mid 0^+_i \rangle \quad ,$$

with $\alpha = (GT,\ F,\ T)$.

Since the transition operator is a two-body one, we may write it as:

$$M^{0\nu}_{\alpha} = \sum_{j_p j_{p'} j_n j_{n'} J_\pi} TBTD\left(j_p j_{p'}, j_n j_{n'}; J_\pi\right) \langle j_p j_{p'}; J^\pi T \mid \tau^-_1 \tau^-_2 O^{\alpha}_{12} \mid j_n j_{n'}; J^\pi T \rangle_a$$

The calculation of the NME

$$M_\alpha^{0\nu} = \sum_{j_p j_{p'} j_n j_{n'} J_\pi} TBTD\left(j_p j_{p'}, j_n j_{n'}; J_\pi\right) \left\langle j_p j_{p'}; J^\pi T \mid \tau_1^- \tau_2^- O_{12}^\alpha \mid j_n j_{n'}; J^\pi T \right\rangle$$

where the two-body transition-density matrix elements are defined as

$$TBTD\left(j_p j_{p'}, j_n j_{n'}; J_\pi\right) = \langle 0_f^+ \mid (a_{j_p}^\dagger a_{j_p'}^\dagger)^{J^\pi} (a_{j_n'} a_{j_n})^{J^\pi} \mid 0_i^+ \rangle$$

and the Gamow-Teller (GT), Fermi (F), and tensor (T) operators as

$$\begin{aligned} O_{12}^{GT} &= \vec{\sigma}_1 \cdot \vec{\sigma}_2 H_{GT}(r) \ , \\ O_{12}^{F} &= H_F(r) \ , \\ O_{12}^{T} &= \left[3\left(\vec{\sigma}_1 \cdot \hat{r}\right)\left(\vec{\sigma}_1 \cdot \hat{r}\right) - \vec{\sigma}_1 \cdot \vec{\sigma}_2\right] H_T(r) \ . \end{aligned}$$

The calculation of the NME

To describe the nuclear properties detected in the experiments, one needs to resort to nuclear structure models.

- Every model is characterized by a certain number of parameters.
- The calculated value of the NME may depend upon the chosen nuclear structure model.

All models may present advantages and/or shortcomings to calculate the NME

The QRPA

The quasiparticle random-phase approximation is based on the concept of “pairing” among the nucleons.

Particles are substituted with “quasiparticles”.

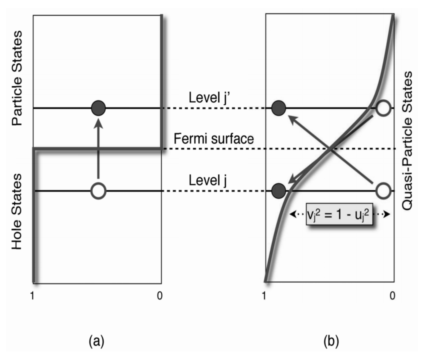

- Advantage $\rightarrow$ The dimension of the hamiltonian does not scale rapidly with the mass number A as with the shell model.
- Shortcoming $\rightarrow$ Results are strongly dependent on the choice of the free renormalization-parameter g_{pp} (g_{ph} is determined from experiment)

The IBM

In the interacting boson model identical nucleons are paired so to generate bosons:

- $L = 0 \rightarrow s$-boson
- $L = 2 \rightarrow d$-boson

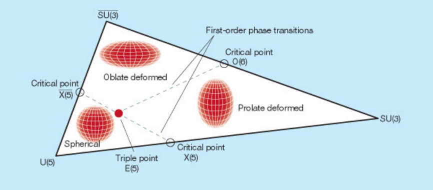

- Advantage $\rightarrow$ The computational complexity is drastically simplified
- Shortcoming $\rightarrow$ The configuration space is strongly reduced

The nuclear shell model

The nucleons are subjected to the action of a mean field, that takes into account most of the interaction of the nucleus constituents.

Only valence nucleons interact by way of a residual two-body potential, within a reduced model space.

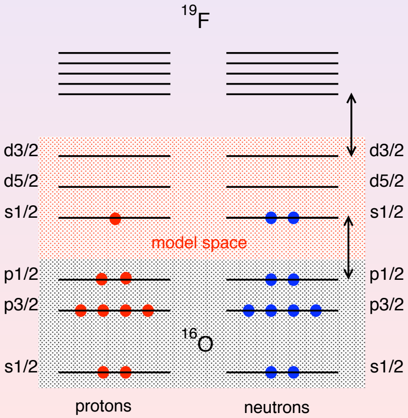

- Advantage → It is a microscopic model, the degrees of freedom of the valence nucleons are explicitly taken into account.
- Shortcoming → High-degree computational complexity.

Nuclear structure calculations

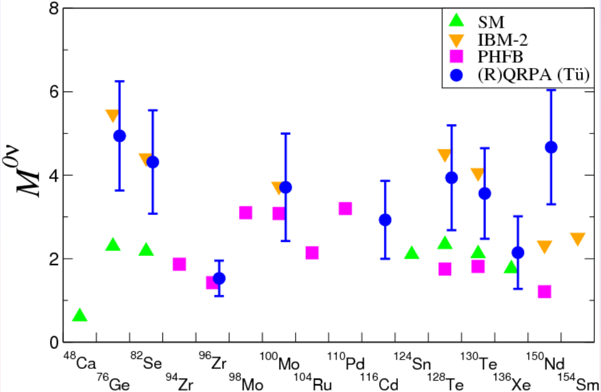

- The spread of nuclear structure calculations evidences inconsistencies among results obtained with different models

The realistic shell model

- The derivation of the shell-model hamiltonian using the many-body theory may provide a reliable approach
- The model space may be “shaped” according to the computational needs of the diagonalization of the shell-model hamiltonian
- In such a case, the effects of the neglected degrees of freedom are taken into account by the effective hamiltonian $H_{\rm eff}$ theoretically

An example: ^{19}F

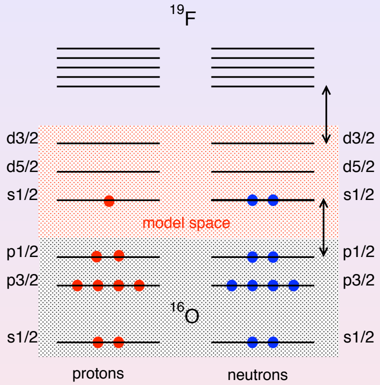

- 9 protons & 10 neutrons interacting
- spherically symmetric mean field (e.g. harmonic oscillator)
- 1 valence proton & 2 valence neutrons interacting in a truncated model space

The degrees of freedom of the core nucleons and the excitations of the valence ones above the model space are not considered explicitly.

Effective shell-model hamiltonian

The shell-model hamiltonian has to take into account in an effective way all the degrees of freedom not explicitly considered

Two alternative approaches

- phenomenological
- microscopic

$$V_{NN} \;\; (+V_{NNN}) \Rightarrow \text{many-body theory} \Rightarrow H_{\rm eff}$$

Definition

The eigenvalues of $H_{\rm eff}$ belong to the set of eigenvalues of the full nuclear hamiltonian

Workflow for a realistic shell-model calculation

1. Choose a realistic *NN* potential (*NNN*)
2. Determine the model space better tailored to study the system under investigation
3. Derive the effective shell-model hamiltonian by way of the many-body theory
4. Calculate the physical observables (energies, e.m. transition probabilities, ...)

Realistic nucleon-nucleon potential: V_{NN}

Several realistic potentials $\chi^2/datum \simeq 1$:
CD-Bonn, Argonne V18, Nijmegen, ...

Strong short-range repulsion

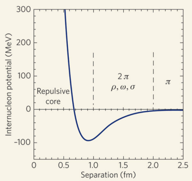

How to handle the short-range repulsion ?

- Brueckner G matrix
- EFT inspired approaches

Realistic nucleon-nucleon potential: V_{NN}

Several realistic potentials $\chi^2/datum \simeq 1$:
CD-Bonn, Argonne V18, Nijmegen, ...

Strong short-range repulsion

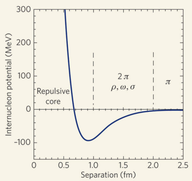

How to handle the short-range repulsion ?

- Brueckner G matrix
- EFT inspired approaches
  - $V_{\text{low-}k}$, SRG
  - chiral potentials

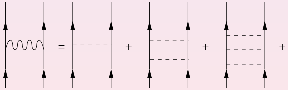

Realistic nucleon-nucleon potential: V_{NN}

Several realistic potentials $\chi^2/datum \simeq 1$:
CD-Bonn, Argonne V18, Nijmegen, ...

Strong short-range repulsion

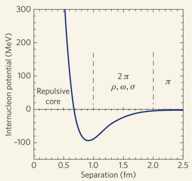

How to handle the short-range repulsion ?

- Brueckner *G* matrix
- EFT inspired approaches
  - $V_{\rm low-k}$, SRG
  - chiral potentials

Realistic nucleon-nucleon potential: V_{NN}

Several realistic potentials $\chi^2/datum \simeq 1$:
CD-Bonn, Argonne V18, Nijmegen, ...

Strong short-range repulsion

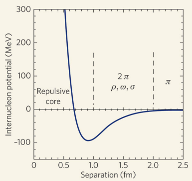

How to handle the short-range repulsion ?

- Brueckner G matrix
- EFT inspired approaches
  - $V_{\mathrm{low-k}}$, SRG
  - chiral potentials

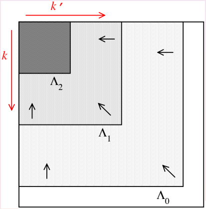

Realistic nucleon-nucleon potential: V_{NN}

Several realistic potentials $\chi^2/datum \simeq 1$:
CD-Bonn, Argonne V18, Nijmegen, ...

Strong short-range repulsion

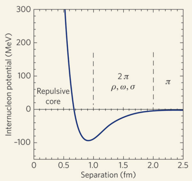

How to handle the short-range repulsion ?

- Brueckner G matrix
- EFT inspired approaches
  - $V_{\mathrm{low-k}}$, SRG
  - chiral potentials

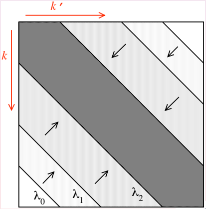

Realistic nucleon-nucleon potential: V_{NN}

Several realistic potentials $\chi^2/datum \simeq 1$:
CD-Bonn, Argonne V18, Nijmegen, ...

How to handle the short-range repulsion ?

- Brueckner G matrix
- EFT inspired approaches
  - $V_{\mathrm{low-k}}$, SRG
  - chiral potentials

Strong short-range repulsion

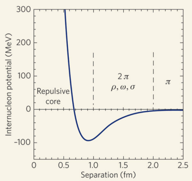

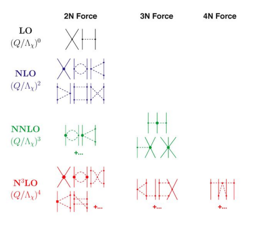

INFN Istituto Nazionale di Fisica Nucleare

The shell-model effective hamiltonian

A-nucleon system Schrödinger equation

$$H|\Psi_\nu\rangle = E_\nu|\Psi_\nu\rangle$$

with

$$H = H_0 + H_1 = \sum_{i=1}^{A}(T_i + U_i) + \sum_{i<j}(V_{ij}^{NN} - U_i)$$

Model space

$$|\Phi_i\rangle = [a_1^\dagger a_2^\dagger \ldots a_n^\dagger]_i|c\rangle \Rightarrow P = \sum_{i=1}^{d}|\Phi_i\rangle\langle\Phi_i|$$

Model-space eigenvalue problem

$$H_{\mathrm{eff}}P|\Psi_\alpha\rangle = E_\alpha P|\Psi_\alpha\rangle$$

The shell-model effective hamiltonian

$$\left(\begin{array}{c|c} PHP & PHQ \\ \hline QHP & QHQ \end{array} \right) \quad \overset{\mathcal{H}=X^{-1}HX}{\underset{Q\mathcal{H}P=0}{\Longrightarrow}} \quad \left(\begin{array}{c|c} P\mathcal{H}P & P\mathcal{H}Q \\ \hline 0 & Q\mathcal{H}Q \end{array} \right)$$

$$H_{\mathrm{eff}} = P\mathcal{H}P$$

Suzuki & Lee $\Rightarrow X = e^{\omega}$ with $\omega = \left(\begin{array}{c|c} 0 & 0 \\ \hline Q\omega P & 0 \end{array} \right)$

$$H_1^{\mathrm{eff}}(\omega) = PH_1P + PH_1Q\frac{1}{\epsilon - QHQ}QH_1P -$$
$$-PH_1Q\frac{1}{\epsilon - QHQ}\omega H_1^{\mathrm{eff}}(\omega)$$

The shell-model effective hamiltonian

Folded-diagram expansion

$\hat{Q}$-box vertex function

$$\hat{Q}(\epsilon) = PH_1P + PH_1Q\frac{1}{\epsilon - QHQ}QH_1P$$

$\Rightarrow$ Recursive equation for $H_{\rm eff}$ $\Rightarrow$ iterative techniques (Krenciglowa-Kuo, Lee-Suzuki, ...)

$$H_{\rm eff} = \hat{Q} - \hat{Q}' \int \hat{Q} + \hat{Q}' \int \hat{Q} \int \hat{Q} - \hat{Q}' \int \hat{Q} \int \hat{Q} \int \hat{Q} \cdots ,$$

The perturbative approach to the shell-model $H^{\rm eff}$

$$\hat{Q}(\epsilon) = PH_1P + PH_1Q\frac{1}{\epsilon - QHQ}QH_1P$$

The $\hat{Q}$-box can be calculated perturbatively

$$\frac{1}{\epsilon - QHQ} = \sum_{n=0}^{\infty} \frac{(QH_1Q)^n}{(\epsilon - QH_0Q)^{n+1}}$$

The diagrammatic expansion of the $\hat{Q}$-box

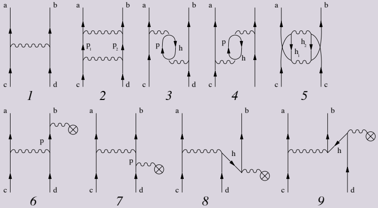

$\hat{Q}$-box perturbative expansion: 1-body diagrams

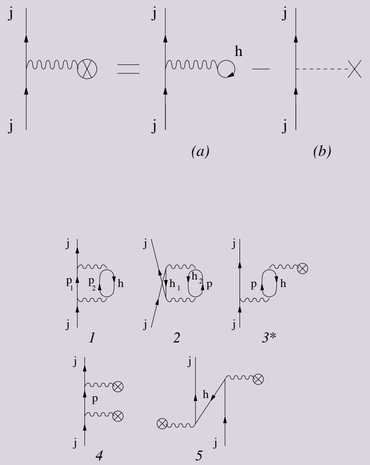

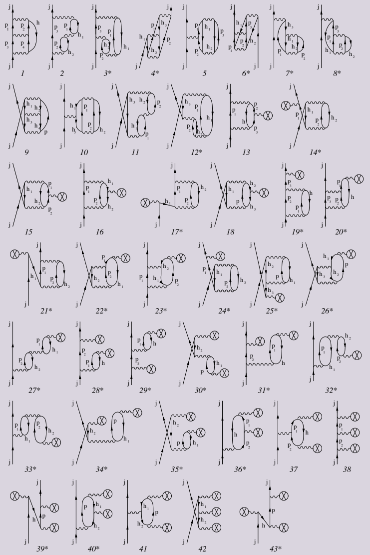

$\hat{Q}$-box perturbative expansion: 2-body diagrams

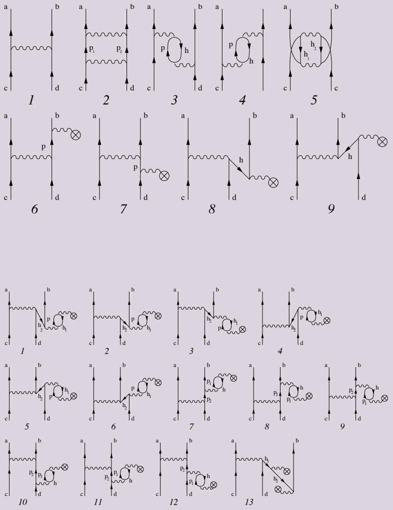

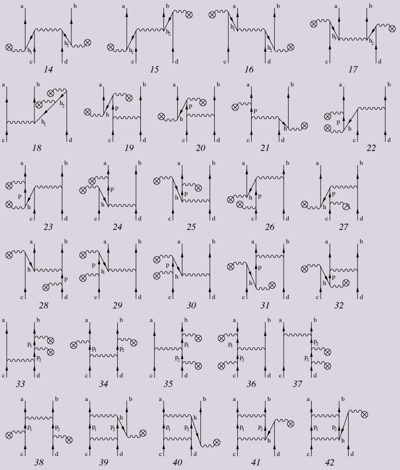

$\hat{Q}$-box perturbative expansion: 2-body diagrams

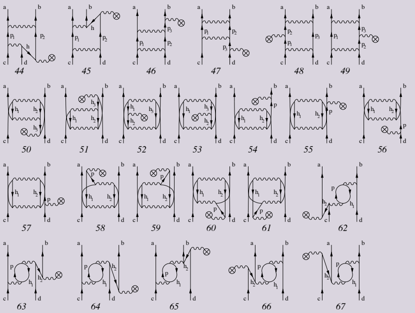

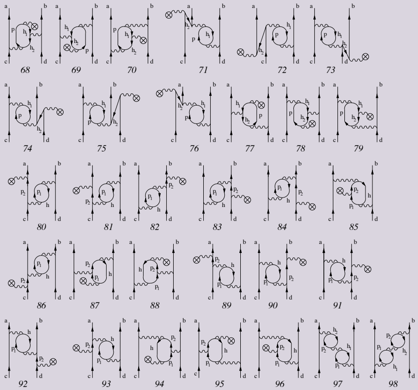

$\hat{Q}$-box perturbative expansion: 2-body diagrams

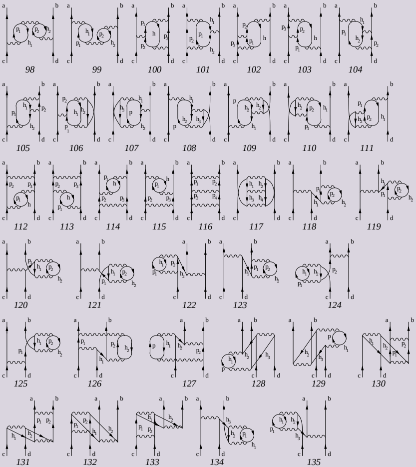

The shell-model effective operators

Consistently, any shell-model effective operator may be calculated

It has been demonstrated that, for any bare operator Θ, a non-Hermitian effective operator $\Theta_{\rm eff}$ can be written in the following form:

$$\begin{aligned}\Theta_{\rm eff} &= (P + \hat{Q}_1 + \hat{Q}_1 \hat{Q}_1 + \hat{Q}_2 \hat{Q} + \hat{Q} \hat{Q}_2 + \cdots)(\chi_0 + \\ &+ \chi_1 + \chi_2 + \cdots) ~,\end{aligned}$$

where

$$\hat{Q}_m = \frac{1}{m!} \frac{d^m \hat{Q}(\epsilon)}{d\epsilon^m} \bigg|_{\epsilon=\epsilon_0} ~,$$

ϵ_0 being the model-space eigenvalue of the unperturbed hamiltonian H_0

The shell-model effective operators

The χ_n operators are defined as follows:

$$
\begin{aligned}
\chi_0 &= (\hat{\Theta}_0 + h.c.) + \Theta_{00} \quad , \\
\chi_1 &= (\hat{\Theta}_1 \hat{Q} + h.c.) + (\hat{\Theta}_{01} \hat{Q} + h.c.) \quad , \\
\chi_2 &= (\hat{\Theta}_1 \hat{Q}_1 \hat{Q} + h.c.) + (\hat{\Theta}_2 \hat{Q} \hat{Q} + h.c.) + \\
& \quad (\hat{\Theta}_{02} \hat{Q} \hat{Q} + h.c.) + \hat{Q} \hat{\Theta}_{11} \hat{Q} \quad , \\
& \quad \ldots
\end{aligned}
$$

and

$$
\begin{aligned}
\hat{\Theta}(\epsilon) &= P \Theta P + P \Theta Q \frac{1}{\epsilon - QHQ} Q H_1 P \quad , \\
\hat{\Theta}(\epsilon_1; \epsilon_2) &= P \Theta P + P H_1 Q \frac{1}{\epsilon_1 - QHQ} \times \\
& \quad Q \Theta Q \frac{1}{\epsilon_2 - QHQ} Q H_1 P \quad ,
\end{aligned}
$$

$$
\hat{\Theta}_m = \frac{1}{m!} \frac{d^m \hat{\Theta}(\epsilon)}{d\epsilon^m} \bigg|_{\epsilon=\epsilon_0} \quad , \quad \hat{\Theta}_{nm} = \frac{1}{n! m!} \frac{d^n}{d\epsilon_1^n} \frac{d^m}{d\epsilon_2^m} \hat{\Theta}(\epsilon_1; \epsilon_2) \bigg|_{\epsilon_1=\epsilon_0, \epsilon_2=\epsilon_0}
$$

The shell-model effective operators

We arrest the χ series at χ_0, and expand it perturbatively:

One-body operator

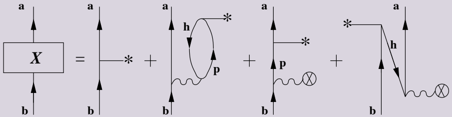

Two-body operator

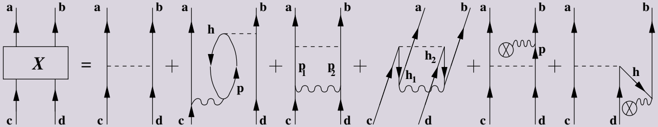

Our recipe for realistic shell model

- Input V_{NN}: $V_{\rm low-k}$ derived from the high-precision *NN* CD-Bonn potential with a cutoff: $\Lambda = 2.6$ fm^{-1}.

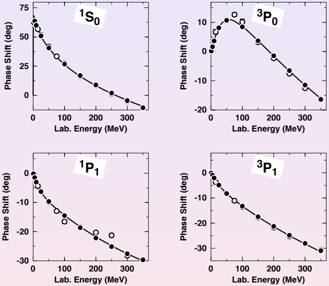

- $H_{\rm eff}$ obtained calculating the *Q*-box up to the 3rd order in perturbation theory.
- Effective operators are consistently derived by way of the the MBPT

Nuclear models and predictive power

Nuclear model $\Rightarrow$ Accurate reproduction of experimental data

$\Downarrow$

Predictive power

Realistic shell-model calculations for ^{130}Te and ^{136}Xe

$\Downarrow$

Check this approach calculating observables related to the GT strengths and $2\nu\beta\beta$ decay and compare the results with data.

$$\left[T_{1/2}^{2\nu}\right]^{-1} = G^{2\nu}\left|M_{2\nu}^{\mathrm{GT}}\right|^2$$

Shell-model calculations for ^{130}Te, ^{136}Xe

PRL **115**, 102502 (2015) PHYSICAL REVIEW LETTERS week ending 4 SEPTEMBER 2015

Search for Neutrinoless Double-Beta Decay of ^{130}Te with CUORE-0

K. Alfonso,[1] D. R. Artusa,[2,3] F. T. Avignone III,[2] O. Azzolini,[4] M. Balata,[3] T. I. Banks,[5,6] G. Bari,[7] J. W. Beeman,[8] F. Bellini,[9,10] A. Bersani,[11] M. Biassoni,[12,13] C. Brofferio,[12,13] C. Bucci,[3] A. Caminata,[11] L. Canonica,[3] X. G. Cao,[14] S. Capelli,[12,13] L. Cappelli,[3,15] L. Carbone,[13] L. Cardani,[9,10,†] N. Casali,[9,10] L. Cassina,[12,13] D. Chiesa,[12,13] N. Chott,[2] M. Clemenza,[12,13] S. Copello,[16,11] C. Cosmelli,[9,10] O. Cremonesi,[13] R. J. Creswick,[2] J. S. Cushman,[17] I. Dafinei,[10] A. Dally,[18] S. Dell'Oro,[3,19] M. M. Deninno,[7] S. Di Domizio,[16,11] M. L. Di Vacri,[3,20] A. Drobizhev,[5,6] L. Ejzak,[18] D. Q. Fang,[14] M. Faverzani,[12,13] G. Fernandes,[16,11] E. Ferri,[12,13] F. Ferroni,[9,10] E. Fiorini,[13,12] S. J. Freedman,[6,5,*] B. K. Fujikawa,[6] A. Giachero,[12,13] L. Gironi,[12,13] A. Giuliani,[21] P. Gorla,[3] C. Gotti,[12,13] T. D. Gutierrez,[22] E. E. Haller,[8,23] K. Han,[17,6] E. Hansen,[24,1] K. M. Heeger,[17] R. Hennings-Yeomans,[5,6] K. P. Hickerson,[1] H. Z. Huang,[1] R. Kadel,[25] G. Keppel,[4] Yu. G. Kolomensky,[5,25] K. E. Lim,[17] X. Liu,[1] Y. G. Ma,[14] M. Maino,[12,13] M. Martinez,[9,26] R. H. Maruyama,[17] Y. Mei,[6] N. Moggi,[27,7] S. Morganti,[10] S. Nisi,[3] C. Nones,[28] E. B. Norman,[29,30] A. Nucciotti,[12,13] T. O'Donnell,[5,6] F. Orio,[10] D. Orlandi,[3] J. L. Ouellet,[5,6] C. E. Pagliarone,[3,15] M. Pallavicini,[16,11] V. Palmieri,[4] L. Pattavina,[3] M. Pavan,[12,13] M. Pedretti,[29] G. Pessina,[13] V. Pettinacci,[10] G. Piperno,[9,10] S. Pirro,[3] S. Pozzi,[12,13] E. Previtali,[13] C. Rosenfeld,[2] C. Rusconi,[13] E. Sala,[12,13] S. Sangiorgio,[29] D. Santone,[3,20] N. D. Scielzo,[29] M. Sisti,[12,13] A. R. Smith,[6] L. Taffarello,[31] M. Tenconi,[21] F. Terranova,[12,13] C. Tomei,[10] S. Trentalange,[1] G. Ventura,[32,33] M. Vignati,[10] S. L. Wagaarachchi,[5,6] B. S. Wang,[29,30] H. W. Wang,[14] L. Wielgus,[18] J. Wilson,[2] L. A. Winslow,[24] T. Wise,[17,18] L. Zanotti,[12,13] C. Zarra,[3] G. Q. Zhang,[14] B. X. Zhu,[1] and S. Zucchelli[34,7]

(CUORE Collaboration)

PRL **109**, 032505 (2012) PHYSICAL REVIEW LETTERS week ending 20 JULY 2012

Search for Neutrinoless Double-Beta Decay in ^{136}Xe with EXO-200

M. Auger,[1] D. J. Auty,[2] P. S. Barbeau,[3,*] E. Beauchamp,[4] V. Belov,[5] C. Benitez-Medina,[6] M. Breidenbach,[7] T. Brunner,[3] A. Burenkov,[5] B. Cleveland,[4,†] S. Cook,[6] T. Daniels,[8] M. Danilov,[5] C. G. Davis,[9] S. Delaquis,[1] R. deVoe,[3] A. Dobi,[9] M. J. Dolinski,[3] A. Dolgolenko,[5] M. Dunford,[10] W. Fairbank, Jr.,[6] J. Farine,[4] W. Feldmeier,[11] P. Fierlinger,[11] D. Franco,[1] G. Giroux,[1] R. Gornea,[1] K. Graham,[10] G. Gratta,[3] C. Hall,[9] K. Hall,[6] C. Hargrove,[10] S. Herrin,[7] M. Hughes,[2] A. Johnson,[7] T. N. Johnson,[12] A. Karelin,[5] L. J. Kaufman,[12] A. Kuchenkov,[5] K. S. Kumar,[8] D. S. Leonard,[13] F. Leonard,[10] D. Mackay,[7,‡] R. MacLellan,[2] M. Marino,[11] B. Mong,[4] M. Montero Díez,[3] A. R. Müller,[3,§] R. Neilson,[3,‖] R. Nelson,[14] A. Odian,[7] I. Ostrovskiy,[3] K. O'Sullivan,[3] C. Ouellet,[10] A. Piepke,[2] A. Pocar,[8] C. Y. Prescott,[7] K. Pushkin,[2] P. C. Rowson,[7] J. J. Russell,[7] A. Sabourov,[3] D. Sinclair,[10,¶] S. Slutsky,[9] V. Stekhanov,[5] T. Tolba,[1] D. Tosi,[3] K. Twelker,[3] P. Vogel,[15] J.-L. Vuilleumier,[1] A. Waite,[7] T. Walton,[6] M. Weber,[1] U. Wichoski,[4] J. Wodin,[7] J. D. Wright,[8] L. Yang,[16] Y.-R. Yen,[9] and O. Ya. Zeldovich[5]

(EXO Collaboration)

- five proton and neutron orbitals outside double-closed ^{100}Sn
  $0g_{7/2}, 1d_{5/2}, 1d_{3/2}, 2s_{1/2}, 0h_{11/2}$
- 1292 two-body matrix elements and 10 SP energies: (I) theoretical SP energies, (II) empirical SP energies fitted to the observed low-lying states in ^{133}Sb and ^{131}Sn

	Proton SP spacings		Neutron SP spacings	
	I	II	I	II
$0g_{7/2}$	0.0	0.0	0.0	0.0
$1d_{5/2}$	0.3	0.4	0.6	0.7
$1d_{3/2}$	1.2	1.4	1.5	2.1
$2s_{1/2}$	1.1	1.3	1.2	1.9
$0h_{11/2}$	1.9	1.6	2.7	3.0

Spectroscopy of ^{130}Te and ^{130}Xe

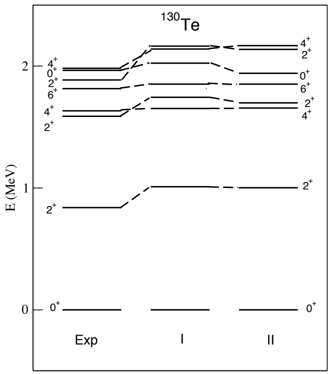

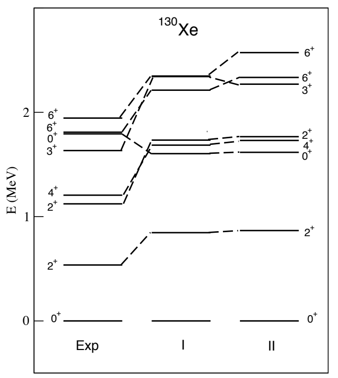

Nucleus	$J_i \rightarrow J_f$	$B(E2)_{Expt}$	I	II
^{130}Te				
	$2^+ \rightarrow 0^+$	580 ± 20	430	420
	$6^+ \rightarrow 4^+$	240 ± 10	220	200
^{130}Xe				
	$2^+ \rightarrow 0^+$	1170^{+20}_{-10}	954	876

Spectroscopy of ^{136}Xe and ^{136}Ba

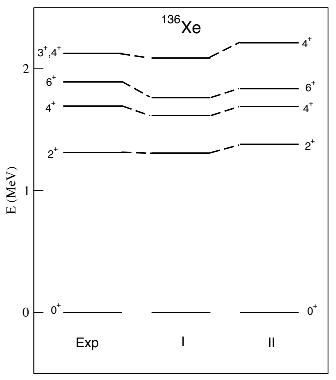

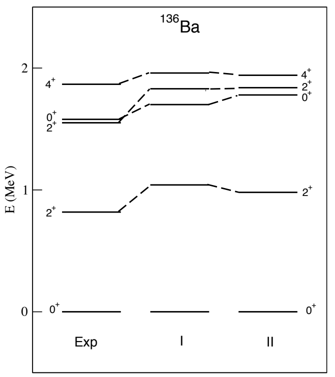

Nucleus	$J_i \rightarrow J_f$	$B(E2)_{Expt}$	I	II
^{136}Xe				
	$2^+ \rightarrow 0^+$	420 ± 20	300	300
	$4^+ \rightarrow 2^+$	53 ± 1	9	11
	$6^+ \rightarrow 4^+$	0.55 ± 0.02	1.58	2.42
^{136}Ba				
	$2^+ \rightarrow 0^+$	800^{+80}_{-40}	590	520

Proton/neutron occupancies/vacancies for $^{130}\mathrm{Te} \rightarrow ^{130}\mathrm{Xe}$

Data from the cross sections of the $(d, ^3\mathrm{He})$ and $(\alpha, ^3\mathrm{He})$

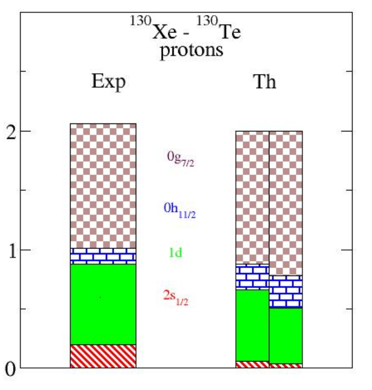

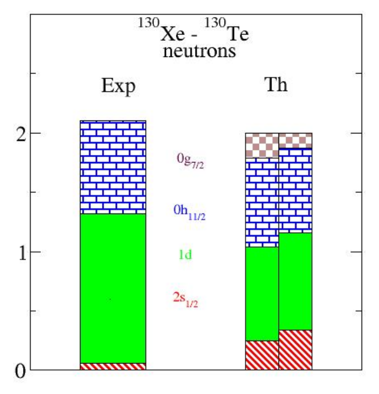

Proton/neutron occupancies/vacancies for $^{136}\mathrm{Xe} \rightarrow {}^{136}\mathrm{Ba}$

Data from the cross sections of the $(d, {}^3\mathrm{He})$ and $(\alpha, {}^3\mathrm{He})$

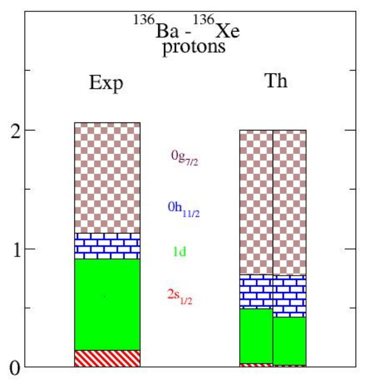

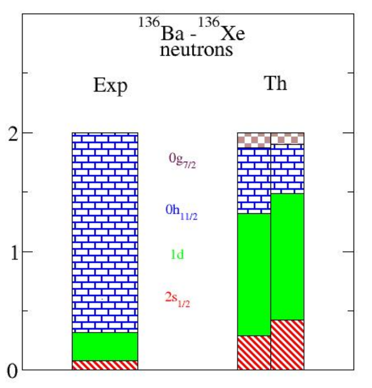

$^{130}\mathrm{Te} \rightarrow ^{130}\mathrm{Xe}$ GT$^-$ running sums

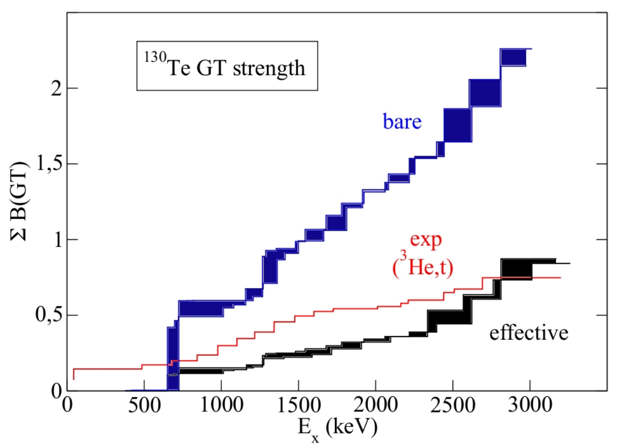

$$B(\mathrm{GT}) = \frac{\left| \langle \Phi_f | \sum_j \vec{\sigma}_j \vec{\tau}_j | \Phi_i \rangle \right|^2}{2J_i + 1}$$

$^{130}\mathrm{Te} \rightarrow {}^{130}\mathrm{Xe}$ nuclear matrix element

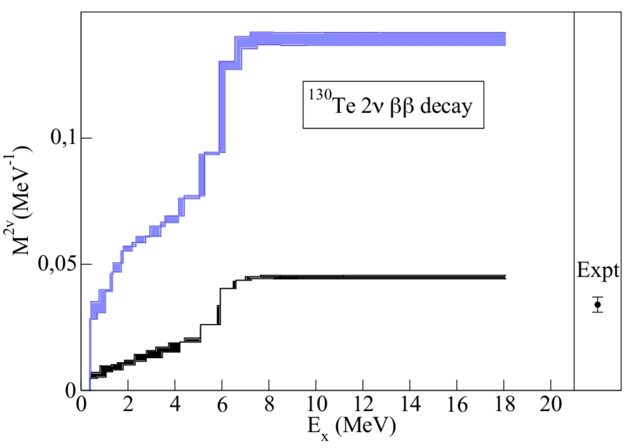

$$M_{2\nu}^{\mathrm{GT}} = \sum_n \frac{\langle 0_f^+ || \vec{\sigma}\tau^- || 1_n^+ \rangle \langle 1_n^+ || \vec{\sigma}\tau^- || 0_i^+ \rangle}{E_n + E_0}$$

^{136}Xe $\rightarrow$ ^{136}Ba GT$^-$ running sums

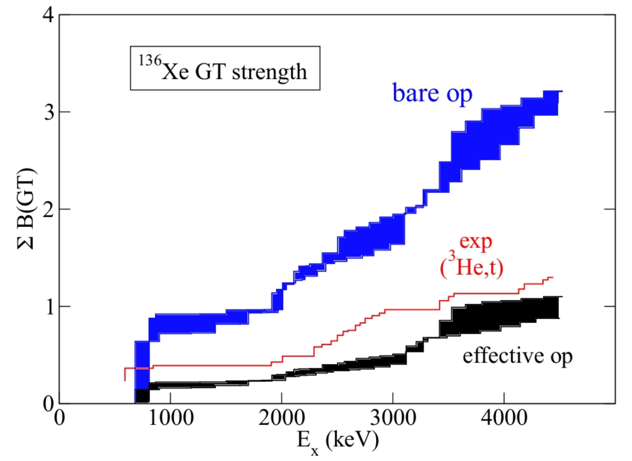

$^{136}Xe \rightarrow ^{136}Ba$ nuclear matrix element

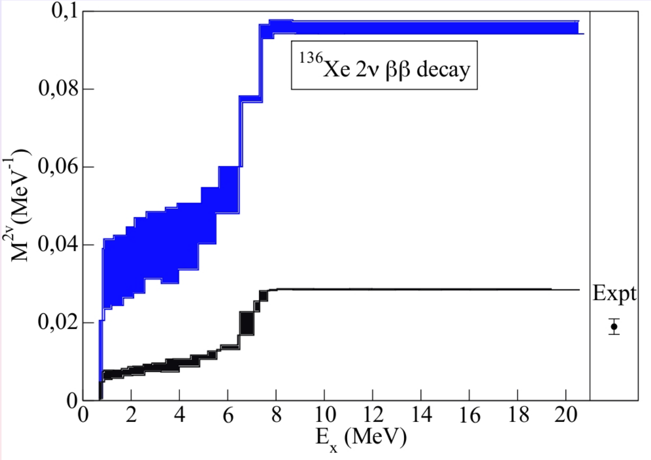

Conclusions and outlook

- The agreement of our results with the experimental data of GT strengths and $2\nu\beta\beta$ NME testifies the reliability of a microscopic shell-model calculation.
- Calculations (I) (all theoretical SM parameters) represents a fully microscopic SM calculation
- We have good prospects of the predictive power of realistic shell model to calculate $0\nu\beta\beta$
- Role of real three-body forces and three-body correlations (blocking effect) should be also investigated.